Geomechanics and Engineering, *Vol. 42, No. 5 (2025) 385-396*
https://doi.org/10.12989/gae.2025.42.5.385

Numerical analysis to assess the bearing capacity of footings in cohesive soil slope under eccentric loading

Khawla Boudiaf[1,2a], Messaoud Baazouzi[1,2a], Nabil Himeur[3,4a], Abdelhakim Bouhadra[1,5a], Abderahmane Menasria[1,5] and Abdelouahed Tounsi*[6]

[1]*Department of Civil Engineering, Abbes Laghrour University Khenchela, BP 1252 Road of Batna, Khenchela 40000, Algeria*
[2]*Laboratory of Research in Civil Engineering (LRGC), University of Biskra, BP14507000 Biskra, Algeria*
[3]*Laboratory of Engineering and Sciences of Advanced Materials, BP 1252 Road of Batna, Khenchela 40000, Algeria*
[4]*Department of Mechanical Engineering, Abbes Laghrour University Khenchela, BP 1252 Road of Batna, Khenchela 40000, Algeria*
[5]*Materials and Hydrology Laboratory, University of Sidi Bel Abbes, Faculty of Technology, Algeria*
[6]*Department of Civil and Environmental Engineering, King Fahd University of Petroleum & Minerals, 31261 Dhahran, Eastern Province, Saudi Arabia*

(*Received May 29, 2025, Revised August 24, 2025, Accepted August 26, 2025*)

Abstract. Foundation stability on sloped terrain in mountainous areas is a key concern in geotechnical engineering. Predicting how these foundations perform under various loads is complex, especially for off-center loaded footings on clay-rich soils. Current analytical approaches often oversimplify soil behavior. This study aims to improve our understanding of the undrained bearing capacity of eccentrically loaded strip footings on cohesive slopes. The research employs finite element limit analysis via OptumG2 software to investigate how load eccentricity direction, normalized crest distance, and soil footing tensile strength affect ultimate bearing capacity. To ensure accuracy, validate the numerical model against established vertical bearing capacity solutions. Our findings reveal intricate relationships among these factors. Eccentric loading significantly impacts bearing capacity, particularly on steeper slopes. The footing's distance from the slope crest is also crucial, with increased stability observed for footings further from the edge. We also noted a non-linear relationship between slope angle and bearing capacity, highlighting the need for conservative design practices on steeper slopes. A new expression that gives an excellent fit to the numerical failure envelope. This work addresses gaps in current knowledge and provides insights for more accurate foundation design in challenging mountainous environments.

Keywords: bearing capacity; eccentric loading; failure mechanism; normalised failure load; load interaction; slope

1. Introduction

In mountain areas, it is a common challenge for geotechnical engineers to assemble all measures necessary for foundation stabilization around slopes. Structures such as pylons, roadways, and bridge supports face climatic loading conditions that could lead to localized failure or instability of a more significant slope. Such events can significantly reduce the load-carrying capacity of a structure and consequently threaten its stability, resulting in more significant environmental damage. (Abdizadeh *et al.* 2021, Acharyya and Dey 2024, Azzouz and Baligh 1983, Baazouzi *et al.* 2023, 2024, Baazouzi *et al.* 2017, Kang *et al.* 2024). Further, the behavior of foundations on slopes is becoming more complex as observed in recent research investigations on different loading and environmental conditions for slope-footing systems (Tan and Vanapalli 2024, Zhang *et al*. 2024).

It's crucial to grasp the intricate interplay between strip footings and slopes to ensure stable foundations. However, the current analytical toolbox - including limit equilibrium, slip line analysis, bound solutions, finite element methods, and discontinuity layout optimization (Bagińska and Srokosz 2019, Fang and Xu 2023, Fang *et al.* 2023, Khasanov and Khasanov 2024, Polishchuk and Semenov 2023, Shohirev *et al.* 2024a, b, Yuan *et al*. 2025, Zhang *et al.* 2023, Zhou *et al.* 2024a, b) often relies on predetermined failure patterns. Recent research has focused on the modeling of orthotropic layered media under mechanical and thermal loads, leveraging analytical methods, finite element analysis (FEM), and hybrid AI techniques. Key contributions include cryogenic contact mechanics in such systems, fatigue and ratcheting behavior in structures, microstructural changes in friction-stir-processed steels, and vibration analysis of piezo-magneto-thermoelastic nanostructures (Yaylacı *et al*. 2024, Fuyad *et al*. 2024, Rajendran *et al*. 2024, Öner *et al.* 2024, Selvamani *et al.* 2024, Yaylacı *et al.* 2023). Neural networks especially multilayer perceptrons are increasingly used alongside FEM and experiments to predict performance and improve modeling accuracy across diverse materials and structural contexts (Yaylacı *et al.* 2025, Aktarer *et al.* 2025, Sekban *et al.* 2024). This reliance may limit the accuracy of our predictions, especially when dealing with complex loading scenarios and the numerous factors that influence how failures occur. Recent progress has attempted to remedy

*Corresponding author, Professor
E-mail: Abdelhakim.bouhadra@univ-khenchela.dz

ISSN: 2005-307X (Print), 2092-6219 (Online)

these shortcomings through novel research avenues such as generalized log-spiral shear mechanisms (Chen and Xiao 2022) or an overall safety zoning methodology (Yuan *et al.* 2025). Contemporary studies have substantially extended the base of our knowledge of the mechanisms of bearing capacity through different analyses. An exact analytical solution for reinforced slopes by using slip line analysis was also developed by (Tarrafa and Hosseininia 2024), in which it was shown that the bearing capacity factor N_γ is a function of soil friction angle, footing setback distance, slope angle, and inclusion layer parameters. Recent studies have shown that loading conditions affect foundation performance. (Saurkar *et al.* 2021) used finite element analysis to study the direction of loads in a foundation. They observed how slope angle, setback ratio, and load direction influence stability in hilly areas. Machine learning studies have gained further evidence of the effect of loading direction and magnitude. (Mustafa *et al.* 2024) assessed loading conditions by evaluating many techniques to predict bearing capacity under inclined loading conditions, and performed a comprehensive analysis to uncover effective modeling to make reliable predictions. Shukla (2024) contributed to the understanding of the seismic bearing capacity of strip footings adjacent to rock slopes by employing an innovative upper-bound finite element limit analysis, utilizing the generalized Hoek-Brown failure criterion for rock strength properties. Innovations in ground improvement have shown remarkable potential to improve foundation performance on slopes. Tafreshi et al. (2025) presented a new ground improvement technique that utilized geogrid-reinforced, densified thin gravel layers. They tested this method in a laboratory, demonstrating significant improvements in the sand-bearing capacity and a reduction in the settlement of the footings. This paper presents enhancements of up to 124%, explains the mechanisms behind the improvement, and demonstrates diminishing returns beyond a specific thickness. Mehrjardi *et al*. (2025) published the results of a numerical simulation of laboratory model tests conducted in FLAC 3D software, providing a solid understanding of the governing mechanics and behavior of shell strip footings placed adjacent to unreinforced and geotextile-reinforced slopes. The unreinforced footing and geogrid-reinforced footing provided the best load-bearing response of the foundation, as they improved the failure mechanism in the slope. Probabilistic approaches have become increasingly common in the discipline to account for uncertainties in soil properties and loading conditions. Choudhuri and Chakraborty (2024) helped develop an understanding of the probabilistic bearing capacity of circular footings on clayey soil (including the influence of spatial variability of undrained shear strength) with numerical analyses (including Monte Carlo simulations) of failure probabilities and the effects of several variables on the bearing capacity factors. Furthermore, Wang *et al*. (2024) also proposed a unique reliability method for evaluating slopes reinforced with anti-sliding piles, particularly for soils exhibiting spatial variability. The study employed a Polynomial Regression model to construct a relationship between the safety factor of the slope system and its key input parameters, demonstrating that the coefficient of variation for the soil strength parameters plays a significant role in controlling slope reliability, outweighing the range of fluctuation. The results, if used wisely, illustrated a disconnect that may exist between the mean of the factor of safety and the actual probability of failure.

Parametric studies on the interactions between geometric parameters and soil properties have obtained some interesting results. (El-Emam *et al.* 2023) have studied the strip footings in cohesiveless slopes using comprehensive finite element analysis and proposed multi-linear equations to estimate bearing capacity in terms of setback distance, internal friction angles, dilatancy angles, footing embedment depth, and width. This information supplements previous research that developed design charts and factors for the bearing capacity of a range of slope shapes. Environmental loading conditions, specifically those related to water infiltration and rainfall, have emerged as essential contributors to the stability of slopes and footings. (Zhang *et al.* 2024) showed that rainfall intensity influences bearing capacity and failure modes more than rainfall patterns, and again emphasizes the necessity of accounting for climatic conditions through lateral earth pressures and other loading to foundation design. Following the work of (Tan and Vanapalli 2022, 2023), who developed estimates of bearing capacity on unsaturated soil slopes undergoing transient flow conditions and had established failure envelopes of footings subjected to inclined and eccentric loading under a range of moisture conditions. This addresses the other part of environmental loads in foundation engineering.

The bearing capacity of expansive soils presents a special source of difficulty. It corresponds with the investigations of (Tan and Vanapalli 2024), who demonstrated that foundation setback, rainfall intensity and duration, and loading conditions significantly impact bearing capacity and slope stability under variable and unusual infiltration scenarios. These studies are particularly relevant for areas where expansive clay soils are found and ultimately affect the soil-structure interaction in more complex ways due to volume changes as moisture fluctuates. Soil improvement and stabilization methods have also been researched to improve foundation performance. So, (Alzabeebee *et al*. 2024) examined the effect of stabilizing a subbase on the bearing capacity of shallow foundations below a footing on clayey soil, making practical recommendations for on-site construction in weak soil foundations. The work done in this area includes research on helical piles in weak soils (Emirler 2024) and sheds light on developing alternative foundation constructions for challenging ground conditions.

Foundation engineering research has increased using numerical models and experimental validation. (Liu *et al.* 2023) conducted experimental and numerical analyses to examine the development of the plastic zone in clay under foundation loads. They validated a numerical model using loading tests in a controlled environment. This work has been critical for comprehending soil-structure interaction and improving design reliability.

We must develop more sophisticated analytical methods to enhance our design practices and deepen our understanding of foundation behavior. These should accurately model how slope foundations respond to loading scenarios, leading to more dependable and cost-effective infrastructure designs in complex mountainous environments. While we have made progress in understanding the undrained bearing capacity of strip footings on cohesive slopes, there's still much to learn about how the direction of load eccentricity (whether positive or negative) interacts with the footing's distance from the slope crest. Our study aims to fill this knowledge gap by examining these factors, soil-footing tensile strength, and their combined effects on bearing capacity. Despite extensive research in foundation stability, we still lack a comprehensive understanding of how eccentrically loaded footings behave near slopes, particularly on cohesive soils. Most previous studies focus more on quite simple methods and on granular soils, which don't depict the inherent complexity of strength in cohesive materials (Turker *et al.* 2014). In other words, investigations into eccentric loading of reinforced and unreinforced sand slopes in such works fail to reflect the specific characteristics of cohesive soil behavior. This research thus seeks to cover these gaps by providing a more in-depth understanding of foundation behavior under the unfavorable aspects of architectural designs. With the help of advanced numerical modeling techniques, the field of analyzing foundation stability has also undergone tremendous improvements. Finite element limit analysis has helped in an in-depth study of foundation behavior on slopes. Different approaches have been used to study this particular problem. For instance, (Georgiadis 2010) used finite element methods to calculate undrained bearing capacity factors, while others have developed design charts for footings on purely cohesive slopes using FELA. Additional research (Shiau *et al.* 2011) studied the stability of the footing on a slope with cohesion and friction, while (Leshchinsky 2015) studied the stability of the footing on c'-φ' slopes, subjecting discontinuity layout optimization. (Xiao *et al.* 2019) applied AFELA to examine the undrained bearing capacity of strip footing on two-layered slopes, and (Cinicioglu and Erkli 2018, Wu *et al.* 2020) proposed the seismic bearing capacity factors for the strip foundations on cohesive slopes. Despite these advances, there is no complete understanding of eccentrically loaded footings on cohesive slopes. It is essential to determine the effect of the direction of load eccentricity (towards or away from the slope face) on the position of the footing relative to the slope crest. This article uses FELA using OptumG2 (Krabbenhoft *et al.* 2015) software to explore the undrained bearing capacity of eccentrically loaded strip footings on slopes and fill that gap. Two eccentricity positions are considered ($e/B = \pm 0.5$): loads shifted away from the slope face and displaced closer to the slope face for different normalized distances from a footing to a sloping crest. By comparing results with existing approaches, their applicability and limitations will be evaluated to understand this vital feature of geotechnical design further. The research aims to furnish engineers in foundation design with the knowledge needed to deal with complicated slope conditions. A new expression that gives an excellent fit to the numerical failure envelope.

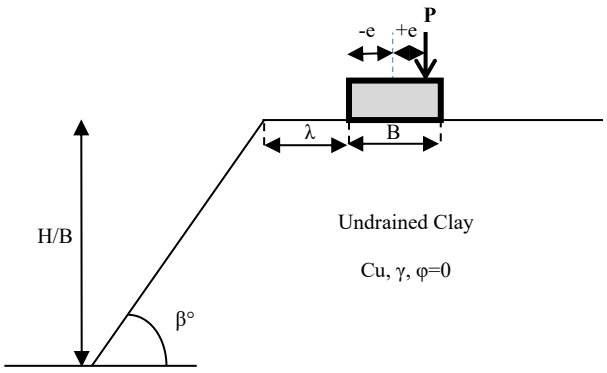

Fig. 1 Problem geometry

2. Problem definition

Fig. 1 shows the geometry of the problem under analysis. In the current study, we consider a rigid strip footing with a width of B=2 m, situated on homogeneous clay soil, and examine the various angles it creates with the horizontal, as well as the slope height H/B=3, at different distances from the foundation's edge to the slope's crest. The soil is modeled as a Tresca material using the Mohr-Coulomb elastic perfectly plastic constitutive model, which impacts the slope's overall stability. The soil has a shear strength C_u (φ=0), an undrained Young's modulus of E_u=22.5 MPa, a Poisson's ratio of ν=0.49, and a unit weight of γ=18 KN/m3. It is assumed that the footing is rigid.

3. Numerical modeling procedure

A finite-element analysis based on the commercial software OPTUM G2 was performed. OPTUM G2 is a two-dimensional program for engineering mechanics computations that simulates the behavior of structures built of soil, rock, or other materials that undergo plastic flow when their yield limits are reached. Many researchers have used the finite element analysis OPTUM G2 to study the bearing capacity of strip and circular footings.

A typical finite element mesh used in the analysis of a 2 m wide footing at a distance of 1*B* m from the crest of a 45 inclination and 3*B* m high soil slope is shown in Fig. 2, Given that the stability of the system is scarcely impacted by slope heights more than 3*B*, the value of *H*/*B* is fixed at 3 to make the analysis easier. Mesh adaptivity is used to avoid the size effect, with shear dissipation as the control variable. According to the software manual, three adaptive iterations are necessary for high accuracy.

The size domain consists of 2,000 elements, corresponding to a 42 m × 15 m wide footing, which minimized the possible

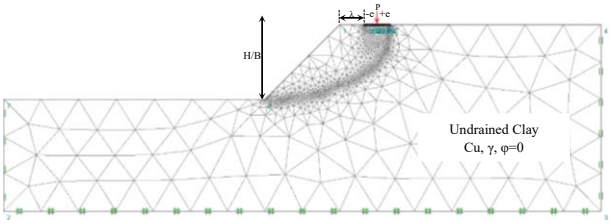

Fig. 2 Problem geometry and Adaptive mesh for β=45° and λ = 1

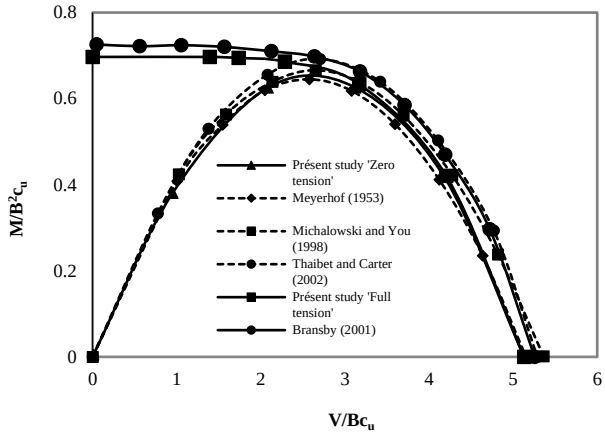

Fig. 3 Non-dimensional failure envelopes in the (V, M) loading plane

boundary effects (the smallest angle of slope of 15° without modifying the overall mesh density). The slope was constructed by excavating the appropriate soil layers for each analysis. The boundary condition for this problem is that the displacement of the left and right vertical sides is constrained in the horizontal direction and is fully fixed to the base of the mesh.

It was assumed that the soil is modeled as a Tresca material using the Mohr-Coulomb elastic-perfectly plastic constitutive model with two shear strengths C_u = 45 and 90 KPa (φ = 0), and the undrained Young's modulus E_u = 22.5 MPa. Poisson's ratio was constant, ν=0.49, to model the undrained conditions with no volume change and ensure numerical stability. The unit weight of soil γ=18 KN/m^3 affects the overall stability of the slope. The footing was assumed to be a rigid plate. The footing is connected to the soil via interface elements. The properties of the interface elements are related to the properties of the adjacent soil elements C=C_u.

4. Results and discussion

4.1 Horizontal ground surface

To validate the numerical model, a comparison was conducted with established solutions for the vertical bearing capacity of strip footings. The numerical simulation yielded a bearing capacity factor (N_c) of 5.19, demonstrating good agreement with Prandtl's theoretical solution of $N_c = \pi + 2$ (Prandtl 1920). The observed discrepancy, with a maximum error of 1%, falls within an acceptable range, confirming the reliability of the chosen modeling approach. While the traditional approach to representing bearing capacity has been through multiplicative factors, recent research has emphasized the use of failure surfaces in load space, also known as load interaction diagrams or normalized failure load envelopes (Fraser Bransby 2001, Gourvenec and Barnett 2011, Michalowski and You 1998, Taiebat and Carter 2002, Ukritchon *et al*. 1998a, b). Fig. 3 presents the non-dimensional failure envelope obtained from the current study, plotted in the (V, M) loading plane. This envelope is compared against those proposed by (Meyerhof 1953, Michalowski and You 1998, Taiebat and Carter 2002) for a footing on a horizontal ground surface. While all failure envelopes exhibit good agreement at lower vertical loads ($V \leq 1.35*B.C_u$), discrepancies emerge at higher vertical loads. The effective width approach proposed by (Meyerhof 1953) consistently underestimates the limit load at higher vertical loads. This discrepancy likely stems from the simplified stress distribution assumptions inherent in the method, which may not accurately capture the complex stress patterns arising at higher vertical loads and in non-homogeneous soil conditions. The analysis reveals that the limit loads predicted by our current study are somewhat lower than those derived from the lower-bound solutions presented by (Michalowski and You 1998, Taiebat and Carter 2002). The maximum differences observed are around 5.78%-4.35%, respectively. This finding is consistent with the general understanding that lower-bound solutions (Fraser Bransby 2001, Houlsby and Puzrin 1999) tend to be conservative, as they are designed to prioritize safety by considering worst-case failure scenarios. A significant outcome of this study is the close correlation with (Meyerhof 1953) regarding the moment capacity of footings. Specifically, it found that the maximum moment capacity occurs at approximately half the ultimate vertical load, 0.5*V_0.

This alignment with previous research, particularly at lower vertical loads, suggests that this model effectively captures the essential load interaction behavior for footings on cohesive slopes. These findings contribute to the ongoing refinement of the understanding of foundation behavior in challenging geotechnical conditions. Comparing present results with established methods and observations can validate the present approach while identifying areas that may offer improved accuracy or insights. This work has important implications for designing and analyzing foundations on sloped terrain, potentially leading to more efficient and reliable engineering solutions.

4.2. Parametric study of influencing factors on bearing capacity

In this part of our study, we examine how various soil and geometric factors influence the maximum load-bearing capacity of strip footings under eccentric loading on inclined surfaces. Our analysis focuses on several critical parameters:

- The ratio of soil cohesion to the product of footing width and soil unit weight
- The relationship between load eccentricity and footing width

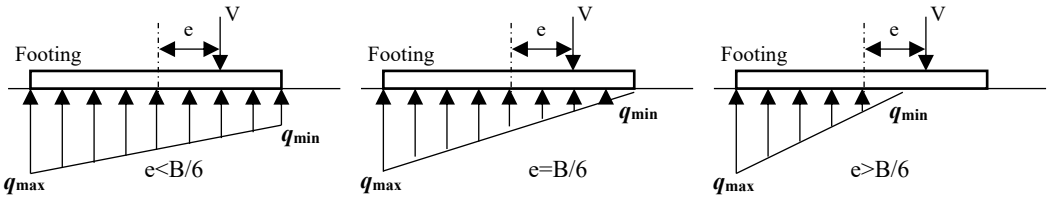

Fig. 4 Distribution of base normal stress at various eccentricities.

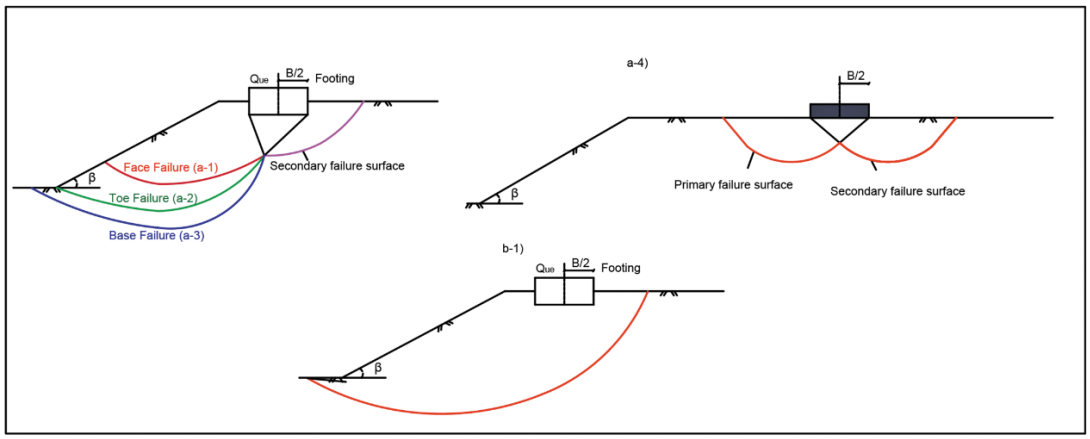

Fig. 5 Different typical failure modes for the footing/slope problem

- The steepness of the slope
- The relative position of the footing to the slope crest

We've designed a systematic approach to evaluate each of these factors independently. Our investigation considers two distinct slope gradients: β = 30-degree incline and a steeper 45-degree slope. Additionally, we explore two scenarios for footing placement: directly at the slope's edge and at a distance equal to the footing's width from the crest. This comprehensive parametric analysis aims to provide insights into how these individual factors and their interactions affect the stability and performance of eccentrically loaded foundations on sloped terrain. Additionally, a range of normalized load eccentricity ratios (e/B) of ± 0.1, 0.2, 0.3, 0.4, and 0.5 is analyzed. As a result, the ultimate bearing capacity would be as follows

$$N_c = \frac{q_u}{c_u} = f\left(\frac{c_u}{\gamma B}, \beta, \lambda, \frac{e}{B}\right) \quad (1)$$

Where q_u is the ultimate bearing capacity of footings, eccentricity e is M/Q, M is the moment, and Q is the vertical load from superstructures. Fig. 4 shows the distribution of base normal stresses at various eccentricities. Typically, a large eccentric load would cause the strip footing to overturn, and in this circumstance, the slope cannot impact the footing. Hence, this study, which builds on the previous one (Duncan *et al.* 1990), attempts to evaluate the first type of load eccentricity e/B between 0 and 0.15. The relationship with both q_{max} and q_{min} in this instance can be represented as follows

$$q_{max} = (12e/B+1)\, q_{min} \quad (2)$$

The maximum base pressure is q_{max}, and the lowest is q_{min}. For a footing-on-slope system, the footings rotate in the direction of the eccentric side or the slope surface, which results in a nonsymmetrical failure mechanism. According to Fig. 3, the eccentric load applied to the slope's right side off the crest is riskier than the left

Furthermore, these parameters are affecting the failure mode of the slope, which can take place according to one of four modes (Zhou *et al.* 2018):

(a-1) In the first failure mode, the face failure

1- mode, the failure slide spreads to the slope face.
2- (a-2) Toe failure mode: a failure surface developed from the footings' back corner to the slope's toe.
3- (a-3) In the base failure mode, a failure slip extends beneath the slope's toe and tends to mobilize more shear resistance than the toe and face failure types. As the slope's influence lessens, the passive resistance recovers.
4- (a-4) Prandtl-type failure mode: A general failure mechanism occurs when a footing is sufficiently removed from the slope crest.

This failure mode is called a "bearing capacity" failure mode. However, the second is:

5- (B-1) overall slope failure, where the critical shear surface involves a portion of the slope and extends
6- beyond the crest.

4.2.1 Influence of the ratio Cu/(γB)

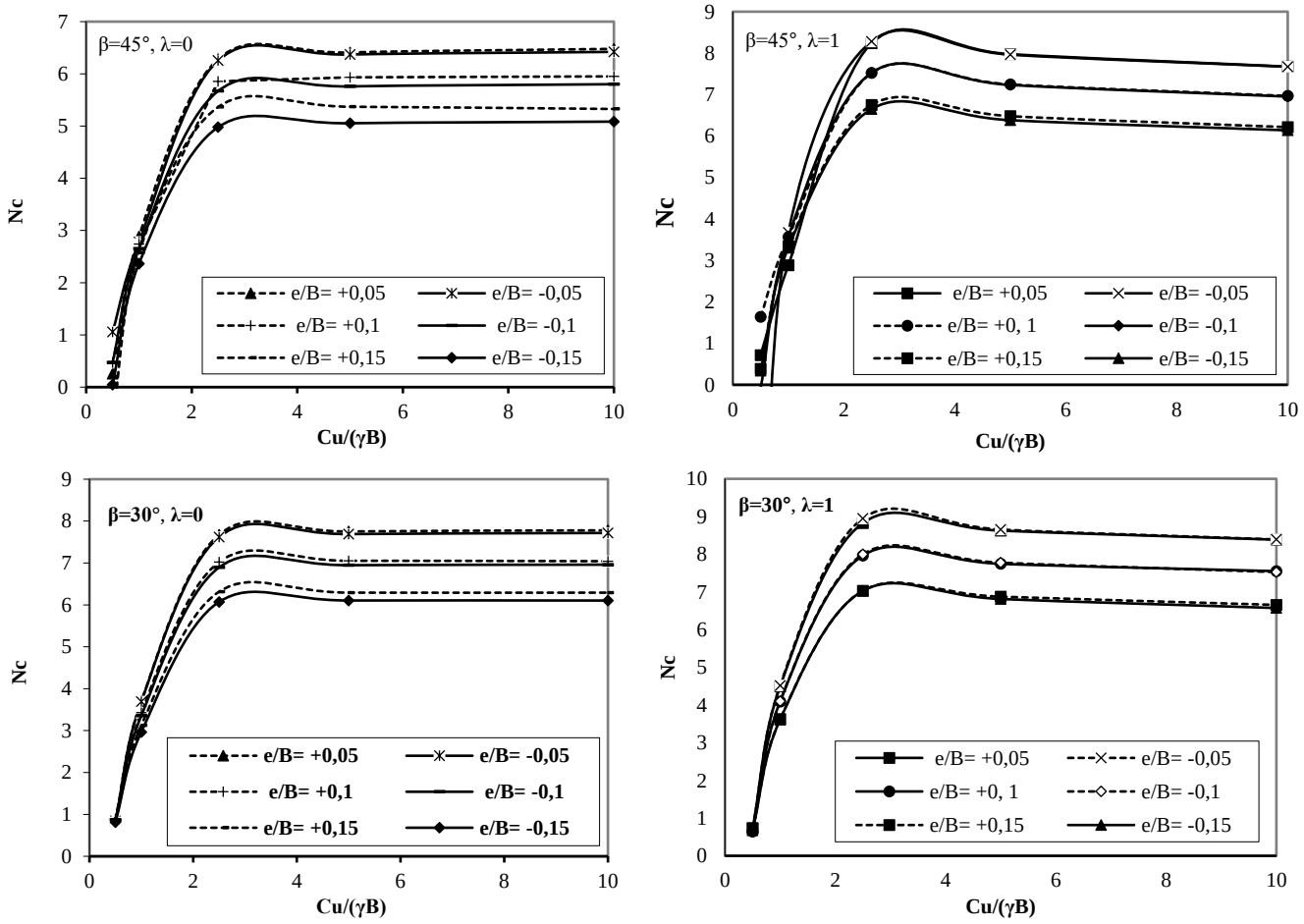

Fig. 6 Impact of shear strength and eccentricity on normalized bearing capacities

For slopes with unit weight γ, a dimensionless strength ratio can be calculated as $C_u/(\gamma B)$. The unit weight γ is a critical component of the footing-on-slope problem, as opposed to its bearing capacity on level ground. In Fig. 5, the effects of strength ratios $C_u/(\gamma B)$ are shown on the undrained bearing capacity of footings resting on slope angles of 15°, 30°, and 45° with normalized distances of 0 and 1 and strengths of 0,5 to 10.

By increasing the strength ratio $C_u/(\gamma B)$, normalized slope/footing distance λ, and slope angle β, the dimensionless bearing capacity N_c increases, which impacts the geometry of the possible failure mechanism at ultimate load. As expected, N_c increases nonlinearly with the strength ratios $C_u/(\gamma B)$ up to a critical $C_u/(\gamma B)$. And the greater $C_u/(\gamma B)$ is, the better the stability becomes once the dimensionless strength ratio exceeds a specific value, $C_u/(\gamma B)$ = 2.5 and 3 for β=30° and 45° respectively, indicating a final transition to the Prandtl-type failure mode with the slope having a negligible impact. The curves indicate identical results for all eccentric loadings for low strength ratio $C_u/(\gamma B) < 1$, demonstrating that the eccentric loading e/B seems to have no effect. This illustrates the complex interaction between footing bearing capacity and slope stability. Furthermore, regarding the eccentricity of the load's behavior, an insignificant reduction in the N_c is observed; a positive eccentricity + (e/B) is more significant than negative eccentricity – (e/B) cases. Moreover, when $C_u/(\gamma B)$ increases, the disparity between cases of symmetrical load eccentricity would increase.

The N_c for normalized distance λ = 1, similar observations to the λ = 0 case can be made for ratios $C_u/(\gamma B)$ = 2.5 to 10. It is noted, however, that in this case, the FELA slightly overestimates the failure loads, indicating that the λ plays an important role when the footing is situated at a distance from the slope. Concerning the behavior of load eccentricity, it can be seen that the bearing capacities of -e/B are identical to the + e/B; moreover, as $C_u/(\gamma B)$ increased, the difference between the two load eccentricities would decrease until these curves overlapped. And because these circumstances overlap, the variation in $C_u/(\gamma B)$ or e/B cannot impact the footing's bearing capacity.

4.2.2 Influence of the ratio Cu/(γB)

The effect of slope angle on the undrained bearing capacity of the foundation near a slope can be illustrated in Fig.7 for $C_u/(\gamma B)$ = 1. Based on the normalized footing distance of 0 to 1, from slope crest to footing crest, we computed the slope angles for 15°, 30°, and 45°. For cases of λ = 0, increasing the value of load eccentricity e/B and β led to a rapid decrease in the undrained bearing capacity factor. The slope angle β affects the bearing capacity factor

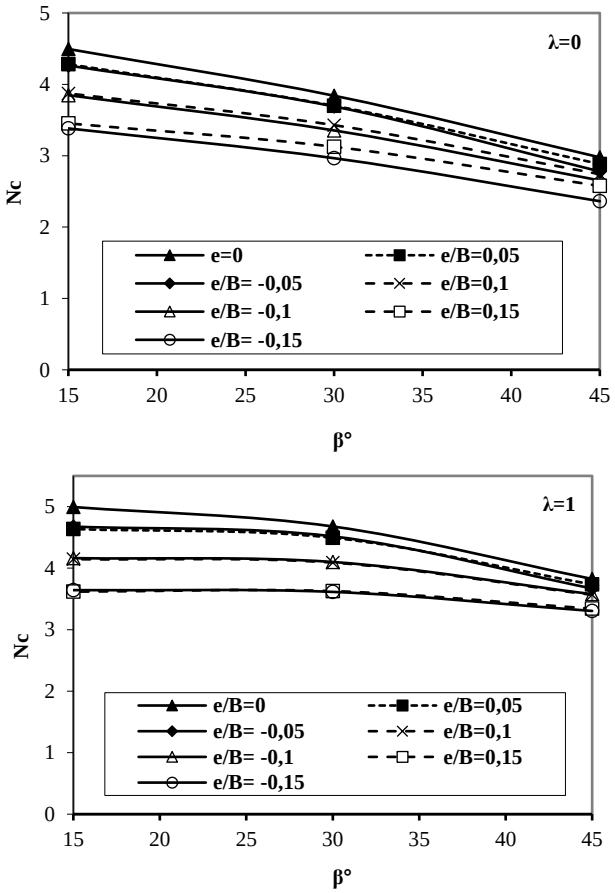

Fig. 7 Impact of slope angle β and eccentricity ratio e/B on normalized bearing capacities

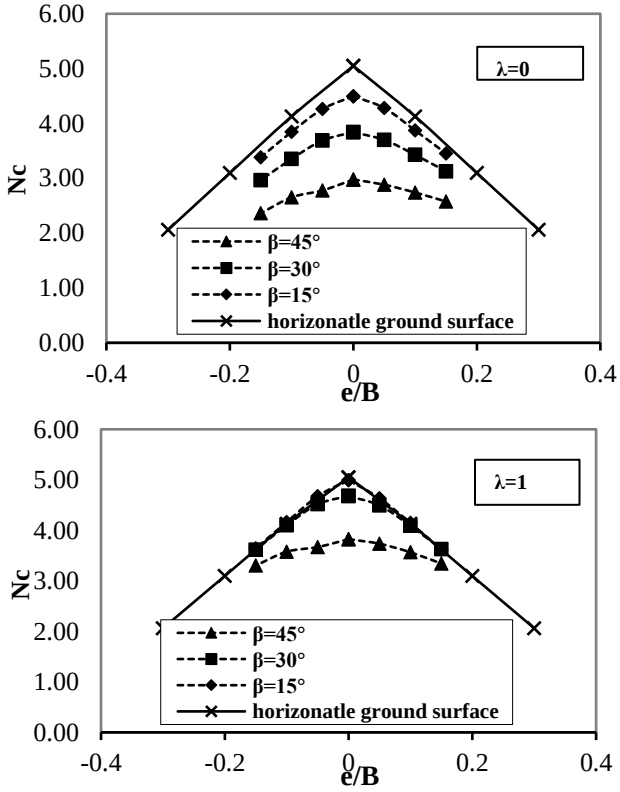

Fig. 8 Impact of eccentricity ratio e/B on bearing capacities for λ=0 and 1

almost linearly. The distance between the strip footing and the slope crest is responsible for increased N_c. As e/B decreases, N_c drops at a different rate. For e/B = 0.1 and 0.15, N_c decreases quickly, ranging from 2.74 to 2.57, and 6.20% for β = 45°. In contrast, β = 30° varies from 3.42 to 3.12, lower by 8.77%. However, for e/B = -0.1 and -0.15, the variation ranges from 2.65 to 2.36, representing a 10.94% decrease at 45°. Similarly, at 30°, the variation ranges from 3.35 to 2.96, corresponding to an 11.64% decrease.

Whereas, for case λ = 1, the bearing capacity decreases, but the N_c reduction rate decreases gradually as the magnitude of β increases. About the behavior of load eccentricity, it can be seen that the bearing capacity of $+e/B$ = (0,05 and 0,1) will remain stable and similar to those of $-e/B$ = (-0,05 and -0,1) for slope angle β = 15° and 30°. Subsequently, it increases faster, in the case of slope angle β = 45°, and the bearing capacities Nc of $-e/B$ are smaller than those of $+e/B$. When e/B = 0.1 and 0.15, the value changes from 3.56 to 3.34, a decrease of 6.17% for 45°. In contrast, for 30°, the value changes from 4.09 to 3.62, a decrease of 11.49%. However, for e/B = -0.1 and -0.15, the range increases from 3.57 to 3.30, decreasing 7.56% for e/B = 45°, and from 4.10 to 3.61, decreasing 11.95% for e/B = 30°. To more intuitively reflect the effect of the slope angle, for λ = 0, a decrease of 8.52%, 3.28%, 3.03% for β = 45°, and 0.27%, 2.33%; and 5.13% for β = 30°, respectively, in the range of $\pm e/B$ (0.05, 0.1; and 0.15). Contrary to this, for slope angles of β = 15° and 30°, the bearing capacities of $+e/B$ are similar to those of $-e/B$. However, when slope angles of β = 45° are considered, the equivalent bearing capacities of $-e/B$ are considerably smaller than those of $+e/B$.

4.2.3 Effect of the eccentric ratio e/B

An analysis of the differences between opposite eccentric directions of the load is performed by evaluating a series of e/B determined graphs. For λ=0, the bearing capacity of some curves is similar. However, the positive eccentric loading is significantly higher than the negative eccentric loading for β=30° and 45°. Due to the small load eccentricity, the footing tilts opposite to the sliding direction caused by the slope, and the slight tilt counteracts the landslide. Due to the combined action of the landslide footing tilt, there would be a continuous declination. In addition, with increasing load eccentricity, the amplitude reductions vary for each side of the load eccentricity. Negative eccentricity has greater reduction gradients than positive eccentricity, and the difference in symmetrical load eccentricity would progressively enlarge as load eccentricity increased. At the same time, the reduction gradients of negative load eccentricity would be gentler for cases of =15°. This phenomenon causes the bearing capacity of e/B = -0.05 to start less than e/B = 0.05 with β = 15°; subsequently, the bearing capacity of e/B = -0.05 would become larger than its symmetrical counterpart as β increases. Considering the variation of normalised distance

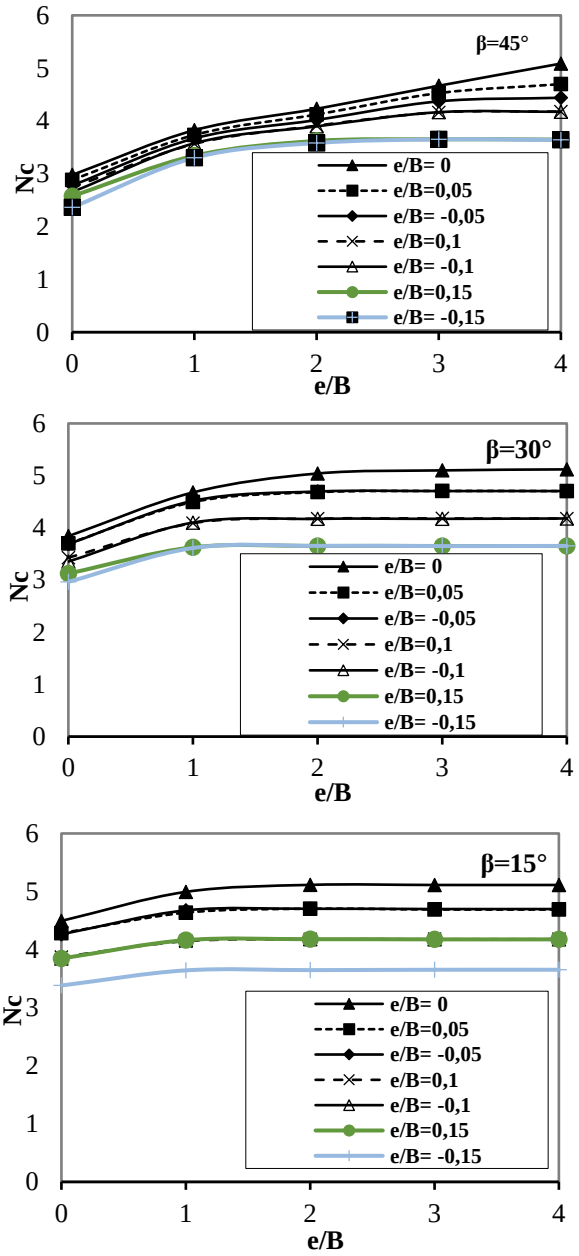

Fig. 9 Impact of λ on bearing capacities for β=45°, 30°, and 15°

λ, since the curves of λ=1 are symmetrical, the horizontal offset of footings would minimize the effects of eccentricity.

4.2.4 Effect of the normalised distance λ

To study the effect of the distance between the footing and the slope crest on the bearing mechanism of the footing, the distance between the footing and the slope crest λ was set as 0, 1, 2, 3, and 4, respectively, for different models. Generally, stability would be better with more λ before the critical distance. Consequently, the slope crest would have a weaker adverse influence on the footing due to its greater distance. The slope is not affected by the edge distance if it is greater than the critical distance. It can be observed that the essential distances for β=45 ° are much larger than those for β=30° and 15°.

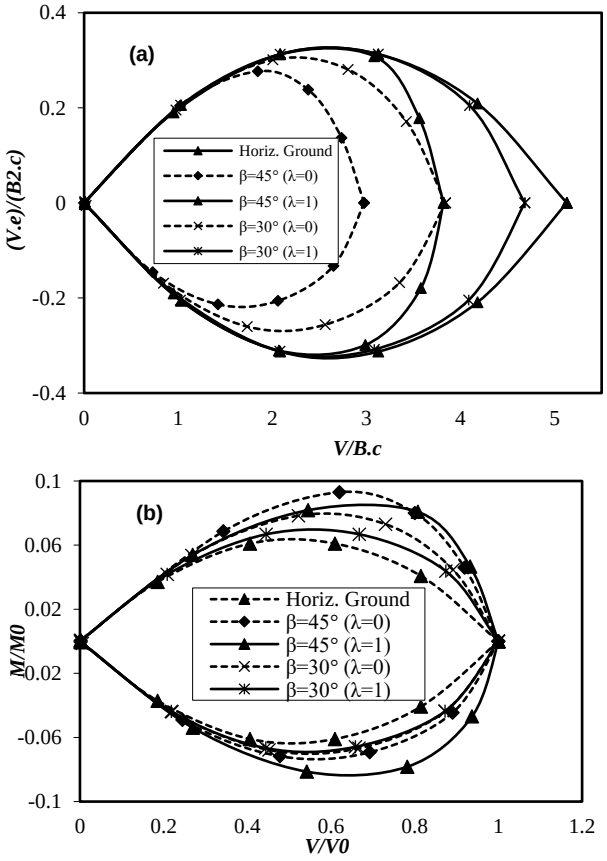

Fig. 10 Normalised failure load (a) and interaction load (b)

Furthermore, the effect of symmetrical load eccentricity becomes less significant, consistent with the view from Fig. 9.

As expected, under the same eccentric loading e/B=0, the critical distances are λ=5,3 and 2, whereas under e/B=0.05, the vital distances λ=4,2 and 1 for β=45°, 30°, and 15°, respectively. This indicates that as edge distance increases, this phenomenon shows that when β increases, the influence scope is wider than when β decreases.

When a footing with an eccentric load is situated on a slope, it tends to rotate in the direction of the eccentric side or the slope surface. This situation will be hazardous if the eccentricity enables the footing to slide towards the slope surface.

4.2.4. Normalized failure load plan and interaction load plan

The results provide valuable insights into the complex interaction of eccentric loading and slope geometry on the bearing capacity of foundations. Using the normalized failure load metric $(V.e)/(B^2.c)$ vs $V/B.c$, the analysis effectively quantifies the impact of load eccentricity and moment on the foundation system. For foundations on horizontal ground, the failure surface exhibits symmetry. However, this symmetry disappears as the slope inclination increases. Notably, the normalized ultimate failure load varied between positive and negative directions for slope inclinations of 45° and 30°. Fig. 10(a) demonstrates that the slope angle has a more pronounced impact at lower eccentricities.

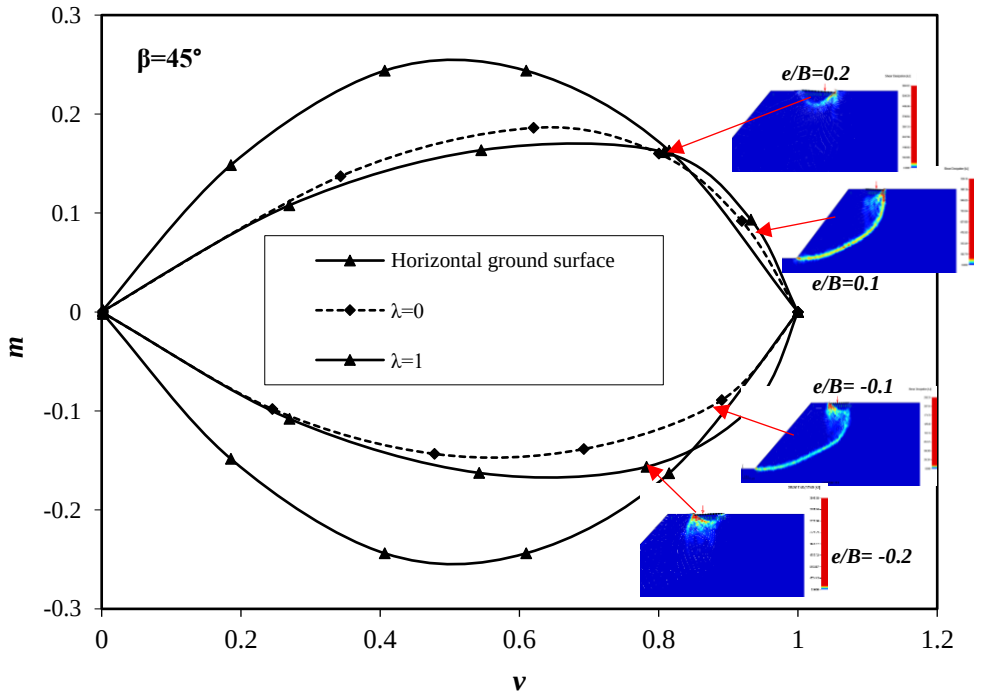

Fig. 11 Eccentric loading that generates the overall slope failure for $\beta = 45$

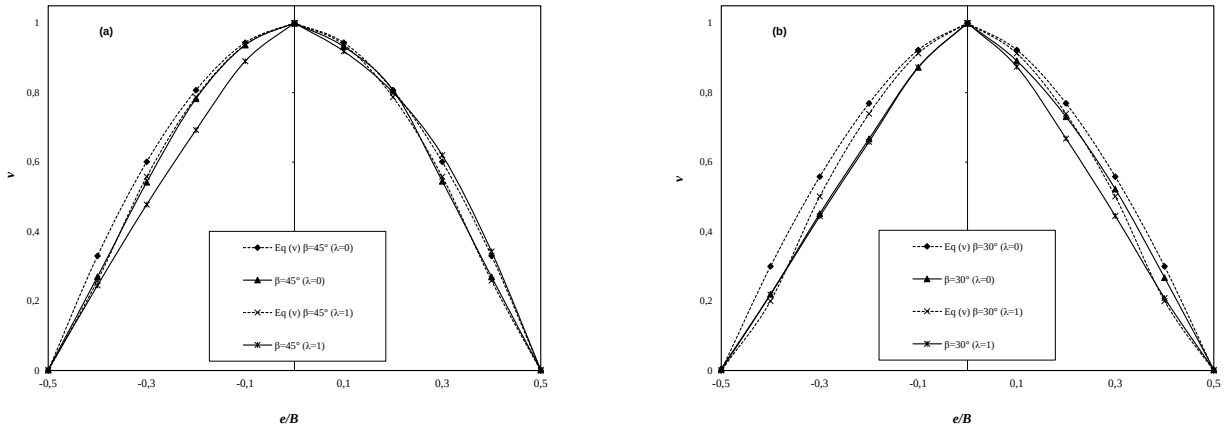

Fig. 12 Effect of eccentricity on load intensity for $\beta = 45°$ and 30°

This suggests that as eccentricity decreases, the destabilizing effect of the slope becomes increasingly significant in determining failure.

For instance, at a foundation located at the crest ($\lambda = 0$), the difference in normalized failure load between $\beta = 30°$ and $\beta = 45°$ is significantly larger at $e/B = 0.1$ compared to $e/B = 0.2$.

Furthermore, at $\lambda = 0$ and $\lambda = 1$, the normalized failure load for $\beta = 45°$ is comparable to that of a horizontal ground surface at $e/B = \pm 0.4$ and ± 0.2, respectively. However, for $\beta = 30°$, this similarity occurs at $e/B = +0.3$ and $+0.2$ for $\lambda = 0$ and 1, respectively, while the corresponding values for negative eccentricities are $e/B = -0.4$ and -0.3, respectively. The interaction load diagrams (M/M_0 vs. V/V_0) presented in Fig.10b offer a practical tool for evaluating bearing capacity under combined loading. An increase in β leads to a steeper interaction curve, particularly in the negative region, signifying a faster reduction in vertical load capacity for a given moment as the slope angle increases.

This underscores the necessity for more conservative design approaches for steeper slopes, especially when considering significant overturning moments. For example, for $\beta = 45°$, the load interaction for $\lambda = 1$ is higher than for $\lambda = 0$ at positive eccentricities ($e/B = +0.1$ and $+0.2$). Conversely, at negative eccentricities ($e/B = -0.1$ to -0.4), the curves indicate a substantial reduction in vertical load capacity, highlighting the increased risk of failure for foundations closer to the crest. Finally, overall slope failure at $\beta = 45°$ for specific eccentricity combinations, as depicted in Fig. 11, highlights a crucial design consideration.

This finding indicates that smaller eccentric loading can influence overall slope failure. Consequently, the slope's effect on eccentric failure loads is less pronounced than its impact on

the ultimate failure load V_o. It follows, therefore, that v may be defined by a new expression that gives an excellent fit to the numerical failure envelope, as follows

$$v = 1 - (e/B)^n * [1 + k \lambda \cos(\beta)] \quad (3)$$

Where: n is a shape factor that depends on β; for β=45°: n= 1.8, for β=30°: n = 1.6 k is a reinforcement influence factor = 0.15.

The Fig. 12. shows the relationship between the slope angle (β) and the adjustment parameter (λ), together with the original and modified values over various e values, which are probably critical variables affecting slope stability. For a slope angle of 45°, Fig. 12(a) employing λ=0, the original and modified values closely converge, with minor differences becoming apparent as e increases. The differences, peaking just under 0.018, suggest that modification slightly favors stability predictions as the slope becomes less stable. As λ ascended from 0 to 1 for the same slope angle, modified values were continuously lower than original values, with differences in the range of 0.005-0.03. This indicates reduced stability due to the adjustment factor, becoming prominent at larger e values.

The results follow a slightly different trend for the slope angle of 30° Fig. 12(b). With λ=0, the modified values are consistently higher than the original ones, with the difference growing from negligible at e=0 to a maximum of approximately 0.035 as e increases. This suggests that the modifications result in more optimistic stability predictions at lower slope angles. When λ=1, the original values decrease more steeply compared to the modified ones as e increases. This results in a more significant discrepancy, up to a maximum difference of approximately 0.1 at higher e values. The trend suggests that the adjustment factor significantly influences stability predictions at higher slope angles and better instability parameters.

5. Conclusions

This paper examined the ultimate bearing capacity of a rigid strip footing on an eccentrically loaded homogeneous clay slope based on the described problem. Using (Krabbenhoft *et al*. 2015) The study used finite element software to investigate the influence of various parameters, such as slope angle, slope-footing distance, and load eccentricity, on the foundation's action. The findings demonstrated that the eccentric loading and the angle of slope interacted with each other in a very complex way, which caused asymmetrical failure in planes and interaction diagrams.

The slope described by eccentricity is more dominant in the angle of the pull-out force, implying a more destabilizing effect as eccentricity decreases.

For non-zero slope angles, the normalized failure load demonstrates asymmetries, emphasizing the slope's influence on the failure behavior.

Flatter or steeper slopes are associated with steeper interaction curves, implying a more rapid decrease in vertical load capacity for a given moment. This research's findings may assist in understanding the load eccentrically mounted on foundations built on slopes. The relations developed between the different characteristic parameters and ultimate bearing capacity would be valuable tools for determining foundation stability under combined loading conditions.

References

Abdizadeh, D., Pakbaz, M.S. and Nadi, B. (2021), "Model test study for dynamic compaction in slope on the bearing capacity of the strip footing", *KSCE J. Civil Eng.*, **25**(5),1700-1704. https://doi.org/10.1007/s12205-021-1409-7.

Acharyya, R. and Dey, A. (2024), "Application of MGGP in Predicting Bearing Capacity of a Strip Footing Resting on the Crest of a Marginal Soil Hillslope", *KSCE J. Civil Eng*., **28**(10), 4244-4257. https://doi.org/10.1007/s12205-024-1217-y.

Aktarer, S.M., Kucukomeroglu, T., Sekban, D.M., Yaylaci, E.U., Yaylaci, M., Ozdemir, M.E. and Mirzaloglu, I. (2025), "Analysis of the changes in microstructure, mechanical, and contact properties of multi-pass friction stir processed DP800 steel", *Adv. Nano Res.*, **18**(3), 253-264. https://doi.org/10.12989/anr.2025.18.3.253.

Alzabeebee, S., Ismael, B.H., Chavda, J.T. and Keawsawasvong, S. (2024), "Effect of subbase stabilization on the bearing capacity of footing resting on clayey soil", *Transport. Infrastruct. Geotechnol*., **11**(5), 3111-3128. https://doi.org/10.1007/s40515-024-00407-5.

Azzouz, A.S. and Baligh, M.M. (1983), "Loaded areas on cohesive slopes", *J. Geotech. Eng*., **109**(5), 724-729. https://doi.org/10.1061/(ASCE)0733-9410(1983)109:5(724).

Baazouzi, M., Khaoula, B., Mohamed, T., Ouassim, R. and Zatar, N. (2024), "Numerical analysis to assess the bearing capacity of footings embedded in cohesive soil slope", *Transport. Infrastruct. Geotech*., **11**(1), 263-282. https://doi.org/10.1007/s40515-023-00280-8.

Baazouzi, M., Mellas, M., Mabrouki, A. and Benmeddour, D. (2017), "Effect of the slope on the undrained bearing capacity of shallow foundation", *Int. J. Eng. Res. Africa*, **28**, 32-44. https://doi.org/10.4028/www.scientific.net/JERA.28.32.

Bagińska, M. and Srokosz, P.E. (2019), "The optimal ANN Model for predicting bearing capacity of shallow foundations trained on scarce data", *KSCE J. Civil Eng*., **23**, 130-137. https://doi.org/10.1007/s12205-018-2636-4.

Chen, T. and Xiao, S. (2022), "Bearing capacity of shallow rigid strip foundations near slopes based on generalized log-spiral shear mechanism".

Choudhuri, K. and Chakraborty, D. (2024), "Probabilistic bearing capacity of circular footing on spatially variable undrained clay", *Geomech. Eng.*, **38**(1), 93-106. https://doi.org/10.12989/gae.2024.38.3.261.

Cinicioglu, O. and Erkli, A. (2018), "Seismic bearing capacity of surficial foundations on sloping cohesive ground", *Soil Dyn. Earthq. Eng*., **111**, 53-64. https://doi.org/10.1016/j.soildyn.2018.04.027.

El-Emam, M., El Berizi, Y., Mabrouk, A.B. and Tabsh, S.W. (2023), "Bearing capacity of strip footing on top of slope: Numerical parametric study", *Ain Shams Eng. J*., **14**(11), 102522. https://doi.org/10.1016/j.asej.2023.102522.

Emirler, B. (2024), "Physical and finite element models for determining the capacity and failure mechanism of helical piles placed in weak soil", *Appl. Sci*., **14**(6), 2389. https://doi.org/10.3390/app14062389.

Fang, H. and Xu, Y. (2023), "New method to evaluate the seismic ultimate bearing capacity of foundations adjacent to slopes considering the dilatancy angle", *Soil Mech. Found. Eng*., **60**(3), 288-295. https://doi.org/10.1007/s11204-023-09893-0.

Fang, H., Xu, Y. and Xu, G. (2023), "New failure mechanism for evaluating the static and seismic ultimate bearing capacity of strip footings adjacent to slope", *KSCE J. Civil Eng.*, **27**(5), 1985-1992. https://doi.org/10.1007/s12205-023-1176-8.

Fraser Bransby, M. (2001), "Failure envelopes and plastic potentials for eccentrically loaded surface footings on undrained soil", Int. J. Numer. Anal. Method. Geomech., **25**(4), 329-346. https://doi.org/10.1002/nag.132.

Fuyad, S.T.M., Al Bari, M.A., Makfidunnabi, M., Nain, H.Z., Özdemir, M.E. and Yaylacı, M. (2024), "Finite element analysis of ratcheting on beam under bending-bending loading conditions", *Struct. Eng. Mech.*, **89**(1), 23-31. https://doi.org/10.12989/sem.2024.89.1.023.

Georgiadis, K. (2010), "Undrained bearing capacity of strip footings on slopes", *J. Geotech. Geoenviron. Eng.*, **136**(5), 677-685. https://doi.org/10.1061/(ASCE)GT.1943-5606.0000269.

Gourvenec, S. and Barnett, S. (2011), "Undrained failure envelope for skirted foundations under general loading", *Géotechnique*, **61**(3), 263-270.

Houlsby, G. and Puzrin, A. (1999), "The bearing capacity of a strip footing on clay under combined loading", *Proceedings of the Royal Society of London. Series A: Mathematical, Physical and Engineering Sciences*, **455**(1983), 893-916. https://doi.org/10.1098/rspa.1999.0340.

Kang, X., Zhu, J. and Liu, L. (2024), "Seismic bearing capacity of strip footings with modified pseudo-dynamic method", *KSCE J. Civil Eng.*, **28**(5), 1657-1674. https://doi.org/10.1007/s12205-024-2479-0

Khasanov, A. and Khasanov, Z. (2024), "Stability of natural slopes and determination of the pressure of incoherent soils on fences", *Soil Mech. Found. Eng.*, **61**(1), 13-19. https://doi.org/10.1007/s11204-024-09937-z.

Krabbenhoft, K., Lyamin, A. and Krabbenhoft, J. (2015), "Optum computational engineering (OptumG2)", Computer software.

Leshchinsky, B. (2015), "Bearing capacity of footings placed adjacent to c′-φ′ slopes", *J. Geotech. Geoenviron. Eng.*, **141**(6), 04015022. https://doi.org/10.1061/(ASCE)GT.1943-5606.0001306.

Liu, X., Jiang, S., Zeng, Y., Hu, W., Gong, Y. and Chen, J. (2023), "The plastic zone of clay under foundation load: an experimental and numerical analysis", *Int. J. Simul. Model.*, **22**(1), 145-156. https://doi.org/10.2507/IJSIMM22-1-CO3.

Mehrjardi, G.T., Khoshnevisan, M. and Sattari, E. (2025), "Numerical modelling on the behavior of strip shell footings placed on reinforced slopes", *Geomech. Eng.*, **40**(5), 323-338. https://doi.org/10.12989/gae.2025.40.5.323.

Meyerhof, G. (1953), "The bearing capacity of foundations under eccentric and inclined loads", *Proceedings of the 3rd ICSMFE*, https://doi.org/https://doi.org/10.3208/sandf1960.11.47.

Michalowski, R.L. and You, L. (1998), "Effective width rule in calculations of bearing capacity of shallow footings", *Comput. Geotech.*, **23**(4), 237-253. https://doi.org/10.1016/S0266-352X(98)00024-X.

Mustafa, R., Samui, P., Kumari, S. and Armaghani, D.J. (2024), "Appraisal of numerous machine learning techniques for the prediction of bearing capacity of strip footings subjected to inclined loading", *Model. Earth Syst. Environ.*, **10**(3), 4067-4088. https://doi.org/10.1007/s40808-024-02008-0.

Öner, E., Yaylacı, E.U. and Yaylacı, M. (2024), "Multi-method examination of contact mechanics in orthotropic layers under gravity", *Mech. Mater.*, **195**, 105036. https://doi.org/10.1016/j.mechmat.2024.105036.

Polishchuk, A. and Semenov, I. (2023), "Calculating the combined foundation settlement for a reconstructed building in clay soils", *Soil Mech. Found. Eng.*, **59**(6), 521-526. https://doi.org/10.1007/s11204-023-09845-8.

Prandtl, L. (1920), "Uber die harte plastischer korper", *Nachr. Ges. Wissensch, Gottingen, math.-phys. Klasse*, 1920, 74-85. https://doi.org/10.1002/zamm.19210010102.

Rajendran, S., Loganathan, R., Yaylaci, M., Yaylaci, E.U. and Ozdemir, M.E. (2024), « Vibration of piezo-magneto-thermoelastic FG nanobeam submerged in fluid with variable nonlocal parameter", *Adv. Nano Res.*, **16**(5), 489-500. https://doi.org/10.12989/anr.2024.16.5.489.

Saurkar, A., Kumar, A., Singh, B. and Mukherjee, M. (2021), "Influence of load inclination on bearing capacity of footing resting on slope", Challenges and Innovations in Geomechanics: *Proceedings of the 16th International Conference of IACMAG-Volume 2 16*, https://doi.org/https://doi.org/10.1007/978-3-030-64518-2_11.

Sekban, D.M., Yaylacı, E.U., Özdemir, M.E., Öztürk, Ş., Yaylacı, M. and Panda, S.K. (2024), "Formability behavior of AH-32 shipbuilding steel strengthened by friction stir process", *Theor. Appl. Fract. Mech.*, **132**, 104485. https://doi.org/10.1016/j.tafmec.2024.104485.

Sekban, D.M., Yaylaci, E.U., Özdemir, M.E. and Yaylaci, M. (2024), « Determination of formability behavior of steel used in ships by various methods", *Struct. Eng. Mech.*, **92**(2), 189-196. https://doi.org/10.12989/sem.2024.92.2.189.

Sekban, D.M., Yaylacı, E.U., Özdemir, M.E., Yaylacı, M. and Tounsi, A. (2025), "Investigating formability behavior of friction stir-welded high-strength shipbuilding steel using experimental, finite element, and artificial neural network methods", *J. Mater. Eng. Perform.*, **34**, 4942-4950. https://doi.org/10.1007/s11665-024-09501-8.

Selvamani, R., Ebrahimi, F., Yaylacı, M., Öztürk, Ş. and Yaylacı, E.U. (2024), "Nonlinear poro-thermo-forced vibration in curved sandwich magneto-electro-elastic shells under hygrothermal environment", *Acta Mechanica*, **235**(9), 5489-5528. https://doi.org/10.1007/s00707-024-03994-z.

Selvamani, R., Thangamuni, P., Yaylacı, M., Emin Özdemir, M., and Yaylacı, E.U. (2024), "Nonlinear vibration and parametric excitation of magneto-thermo elastic embedded nanobeam using homotopy perturbation technique", *ZAMM-J. Appl. Math. Mech. Zeitschrift für Angewandte Mathematik und Mechanik*, **104**(12), e202400525. https://doi.org/10.1002/zamm.202400525.

Shiau, J., Merifield, R., Lyamin, A. and Sloan, S. (2011), "Undrained stability of footings on slopes", *Int. J. Geomech.*, **11**(5), 381-390. https://doi.org/10.1061/(ASCE)GM.1943-5622.0000092.

Shohirev, M., Karaulov, A. and Korolev, K. (2024a), "Calculation of the bearing capacity of a two-layer soil base under an inclined load", *Soil Mech. Found. Eng.*, **60**(6). https://doi.org/10.1007/s11204-024-09922-6.

Shohirev, M., Karaulov, A. and Korolev, K. (2024b), "Calculation of the bearing capacity of a two-layer soil base under an inclined load", S*oil Mech. Found. Eng.*, **60**(6), 509-513.

Shukla, R.P. and Basudhar, P.K. (2024), "Seismic bearing capacity of skirted footings using finite element analysis", *Geomech. Eng.*, **39**(1), 13-26. https://doi.org/10.12989/gae.2024.39.1.013.

Taiebat, H. and Carter, J. (2002), "Bearing capacity of strip and circular foundations on undrained clay subjected to eccentric loads", *Géotechnique*, **52**(1), 61-64. https://doi.org/10.1680/geot.2002.52.1.61.

Tafreshi, S.M., Balf, H.A., Rezaeinejad, H.R., O'Kelly, B.C. and Faramarzi, A. (2025), "Bearing pressure enhancement of sand foundation beds by encapsulating geogrids in thin densified gravel layer inclusions", *Geomech. Eng.*, **40**(4), 277-293. https://doi.org/10.12989/gae.2025.40.4.277.

Tan, M. and Vanapalli, S.K. (2022), "Foundation bearing capacity estimation on unsaturated soil slope under transient flow

condition using slip line method", *Comput. Geotech*., **148**, 104804. https://doi.org/10.1016/j.compgeo.2022.104804.

Tan, M. and Vanapalli, S.K. (2023), "Failure envelops for foundation subjected to inclined and eccentric loading considering steady state and transient flow conditions in unsaturated soils", *Comput. Geotech.*, **157**, 105315. https://doi.org/10.1016/j.compgeo.2023.105315.

Tan, M. and Vanapalli, S.K. (2024), "Shallow foundation behavior on an expansive soil slope subjected to different infiltration conditions", *Can. Geotech. J.*, **61**(10), 2286-2303. https://doi.org/10.1139/cgj-2023-0184.

Tarrafa, M. and Hosseininia, E.S. (2024), "The exact bearing capacity of strip footings on reinforced slopes using slip line method", *Geomech. Eng*., **38**(3), 261-273. https://doi.org/10.12989/gae.2024.38.3.261.

Ukritchon, B., Whittle, A.J. and Sloan, S.W. (1998a), "Undrained limit analyses for combined loading of strip footings on clay", *J. Geotech. Geoenviron. Eng*., **124**(3), 265.

Ukritchon, B., Whittle, A.J. and Sloan, S.W. (1998b), "Undrained limit analyses for combined loading of strip footings on clay", *J. Geotech. Geoenviron. Eng*., **124**(3), 265-276. https://doi.org/10.1061/(ASCE)1090-0241(1998)124:3(265).

Wang, Y., Shang, H., Wan, Y. and Yu, X. (2024), "Reliability analysis of soil slope reinforced by micro-pile considering spatial variability of soil strength parameters", *Geomech. Eng*., **36**(6), 631-640. https://doi.org/10.12989/gae.2024.36.6.631Wu, G., Zhao, H., Zhao, M. and Xiao, Y. (2020), "Undrained seismic bearing capacity of strip footings lying on two-layered slopes". *Comput. Geotech.*, **122**, 103539. https://doi.org/10.1016/j.compgeo.2020.103539.

Xiao, Y., Zhao, M., Zhang, R., Zhao, H. and Wu, G. (2019), "Undrained bearing capacity of strip footings placed adjacent to two-layered slopes", *Int. J. Geomech*., **19**(8), 06019014. https://doi.org/10.1061/(ASCE)GM.1943-5622.0001480.

Yaylacı, M., Öner, E., Adıyaman, G., Öztürk, Ş., Uzun Yaylacı, E. and Birinci, A. (2023), "Analyzing of continuous and discontinuous contact problems of a functionally graded layer: theory of elasticity and finite element method", *Mech. Based Des. Struc*., **52**(8), 5720-5738. https://doi.org/10.1080/15397734.2023.2262562.

Yaylacı, M., Yaylı, M., Öztürk, Ş., Ay, S., Özdemir, M.E., Yaylacı, E.U. and Birinci, A. (2024), "Examining the contact problem of a functionally graded layer supported by an elastic half-plane with the analytical and numerical methods", *Math. Method. Appl. Sci*., **47**(12), 10400-10420. https://doi.org/10.1002/MMA.10129.

Yaylaci, M., Yaylaci, E.U., Turan, M., Ozdemir, M.E., Ozturk, S. and Ay, S. (2024), "Research of the crack problem of a functionally graded layer", *Steel Compos. Struct*., **50**(1), 77-87. https://doi.org/10.12989/scs.2024.50.1.077.

Yaylacı, M., Yazıcıoğlu, A., Yaylacı, E.U., Terzi, M. and Birinci, A. (2025), "Evaluation of the contact problem of two layers one of functionally graded, loaded by circular rigid block and resting on a Pasternak foundation by analytical and numerical (FEM and MLP) methods", *Arch. Appl. Mech*., **95**(4), 1-23. https://doi.org/10.1007/s00419-025-02787-7.

Yuan, H., Xiao, Q., Xiao, Y., Dang, L., Qiu, Z., Han, X., Zhang, M., Zhu, Z. and Liu, J. (2025), "Bearing capacity and safety zoning of strip footings near slopes considering slope Stability". *Geotech. Geol. Eng*., **43**(5), 1-21. https://doi.org/10.1007/s10706-025-03151-w.

Zhang, J., Wang, T., Wu, H., Yuan, Y. and Zhou, A. (2023), "Remote boundary for numerical simulations of soil slope response to earthquakes", *Soil Mech. Found. Eng*., **60**(5), 459-465. https://doi.org/10.1007/s11204-023-09915-x.

Zhang, W., Gu, X. and Ou, Q. (2024), "Bearing capacity and failure mechanism of strip footings lying on slopes subjected to various rainfall patterns and intensities", *Geol. J*., **59**(9), 2371-2382. https://doi.org/10.1002/gj.4882.

Zhou, H., Zheng, G., Yin, X., Jia, R. and Yang, X. (2018), "The bearing capacity and failure mechanism of a vertically loaded strip footing placed on the top of slopes", Comput. Geotech., **94**, 12-21. https://doi.org/10.1016/j.compgeo.2017.08.009.

Zhou, Y., Shi, S. and Cai, Q. (2024a), "A model test and the ultimate capacity analysis of multi-underreamed anchors in silty clay", *Soil Mech. Found. Eng*., **60**(6), 564-573. https://doi.org/10.1007/s11204-024-09930-6.

Zhou, Y., Shi, S. and Cai, Q. (2024b), "A model test and the ultimate capacity analysis of multi-underreamed anchors in silty clay", *Soil Mech. Found. Eng*., 1-10. https://doi.org/10.1007/s11204-024-09930-6.

CC